EINDHOVEN UNIVERSITY OF TECHNOLOGY

Utrecht University

Master's Programme in Theoretical Physics
Theory for Technology course, 7.5 ECTS

Computational modelling of nanowire growth

Author: Juan José Rodríguez,
Institute for Theoretical Physics, Utrecht University

Supervisors: Prof. Erik Bakkers,
Orson van der Molen,
Department of Applied Physics, Eindhoven University of Technology
Prof. Rembert Duine,
Institute for Theoretical Physics, Utrecht University

Abstract

Devices composed of semiconducting nanowires present a wide variety of potential applications in both technology and science. Their small size allows for the development of structures at the nanoscale, as well as the exploitation of the quantum effects that naturally manifest in that realm. Because of these reasons and more, there is a great deal of interest in studying how to efficiently grow them in laboratories.

Many of the potential applications enabled by semiconducting nanowires consist in increasing the efficiency of technologies that already exist today, such as solar photovoltaic energy production or atomic force microscopy. However, they can also pave the way for innovative technologies in the fields of quantum photonics and computing. For example, one of the most interesting applications in that regard is their use for the development of quantum bits or qubits. These qubits would take advantage of the quantum nature of the nanowires placed in a certain environment. In particular, it is expected that under the right conditions two quantum states, called Majorana zero modes, manifest at the two tips of the nanowire. These elusive states should be able to store quantum information in a way that is resistant to external noise, and that could allow for its processing in a paradigm called topological quantum computation.

Semiconducting nanowires are grown in laboratories in both academy and industry by means of different procedures. The most widely used procedure is the vapour-liquid-solid method (VLS), in which a liquid catalyst material (usually a droplet of gold) is placed between the vapour and the crystalline phases of the semiconductor material in order to accelerate the reaction. However, there may be limitations when growing nanowires with this procedure, especially with respect to scalability. An alternative and potentially more scalable procedure is selective area epitaxy (SAE), in which nanowires are grown over a semiconducting substrate coated with a dielectric mask with openings or trenches which expose the underlying material. Nanowires grown using this procedure show show growth regimes which have been experimentally observed. In one of these, the nanowires compete with each other for the material, while on the other they share the material between them through diffusive mechanisms. These regimes could be used as a way to understand the microscopic mechanisms that govern nanowire growth, and therefore, lead to a better understanding of them.

The objective of this work is to numerically model the growth of nanowires coming from selective area epitaxy. The different growth regimes will be explored as a function of the numerical parameters employed, hopefully leading to some qualitative insights.

Contents

1 Introduction

1.1 Background

Semiconducting nanowires are small crystalline filaments composed of a semiconductor material and with diameters in the order of a few nanometres, typically between 20 and 200nm. The most commonly used materials are type III-V semiconductors, such as GaAs, InP or InAs because of their superior electronic properties, although it is also possible to create nanowires from other materials. They are grown and studied in both academic and industrial settings, by means of very valuable and specialized machinery in order to reach the challenging experimental conditions needed for their growth.

These nanowires present a wide variety of applications due to their small diameter, in part because it allows for the manifestation of exotic quantum effects. By their means, it is possible to achieve crystalline phases for the semiconductors that are impossible to achieve under normal conditions [1]. Also, and as the first example of their applications, they can be used to increase the efficiency in photovoltaic devices [2]. In addition, they can be used to build nanoscale lasers which allow for the construction of optical structures with applications in both classical and quantum computing [3].

1.2 The Majorana chain

Semiconducting nanowires have a very promising future in the field of quantum computation and information processing. By means these nanowires, it may be possible to experimentally implement a, for now, theoretical model within condensed matter physics known as the Majorana chain. It was proposed by Alexei Kitaev in 2001, and it is one of the first theoretical models to possess a so-called topological phase [4]. In this case, the topological phase implies the emergence of two zero-energy and charge-neutral quasiparticles called Majorana zero modes at the edges of the system. These quasiparticles are the condensed matter analogues of the yet theoretical Majorana fermions, hypothesized by Ettore Majorana in 1937 with the fundamental property that they are their own antiparticle[5].

The Majorana chain consists of a collection of N immobile fermions, such as electrons, restrained to stay in one dimension and interacting with each other via a nearest-neighbour interaction, that is, only with the closest electrons in each of the two directions. This allows for the interaction to be modelled only by pair terms, and gives place to a quantum many-body hamiltonian of the form

$$H = \sum_{n=1}^{N-1} \left[t\left(f_n^\dagger f_{n+1} + f_n f_{n+1}^\dagger\right) + \left(\Delta f_n^\dagger f_{n+1}^\dagger + f_n f_{n+1}\right)\right] - \sum_{n=1}^{N} \mu\left(f_n^\dagger f_n + f_n f_n^\dagger - 1\right), \qquad (1.1)$$

where f_n and $f_n^\dagger$ are, respectively, the fermionic creation and annihilation operators. These operators represent mathematically the creation or destruction of an electron at site $n \in N$. The parameter t corresponds to the nearest-neighbour hopping amplitude, as it is coupled to terms of the form $f_n^\dagger f_{n+1}$ and $f_n f_{n+1}^\dagger$ which represent the quantum transition amplitude for the electron to "hop" between the sites n and $n+1$. On the other hand, Δ is an s-wave superconducting pairing term as it is coupled to terms $f_n^\dagger f_{n+1}^\dagger$ representing the creation and annihilation of Cooper pairs, and $f_n^\dagger f_{n+1}^\dagger$ representing their annihilation. Finally, μ is a chemical potential coupled to the number operator $\hat{N} \equiv f_n^\dagger f_n$. Such a chemical potential is usually caused by an external magnetic field.

The Majorana chain is an example of a quantum system which is said to be strongly correlated, meaning that it is very difficult to solve. However, there is a way do it by means of a well known mathematical identity, called the Jordan-Wigner transformation, which allows us to transform it into a one-dimensional chain of spins. This transformation is highly non-local in the sense that it relates every single spin with *all* the electrons in the Majorana chain at once. Even though the resulting spin chain does not represent the original model, and the degrees of freedom seem to have become *unphysical* after such a convoluted and highly non-local transformation, the resulting chain is way easier to solve. In some cases, for example when setting $\Delta = t$, it is even analytically solvable. We can then use the analytical solution to study the phases of the Majorana chain.

Setting $\Delta = t$ in (1.1), the resulting spin is called the transverse-field Ising model (1.2). It is a quantum generalization of the classical Ising model used to model magnetism in statistical mechanics, and one of the first models ever discovered to show a phase transition[6]. It is composed of a collection of spin one-half particles with nearest-neighbour interactions together with an oriented magnetic field $\frac{\mu}{2t}$ which forces the spins to align in its direction.

$$H = -t \sum_i \left(\sigma_i^x \sigma_{i+1}^x - \frac{\mu}{2t} \sigma_i^z \right). \tag{1.2}$$

The transverse-field Ising model presents a ferromagnetic phase when the magnetic field $\frac{\mu}{2t}$ is smaller than one. In that phase, the spins are disordered and, on average, do not align in a particular direction. The corresponding phase for the Majorana chain is a trivial band insulator with gap μ. On the other hand, for a magnetic field $\frac{\mu}{2t}$ greater than one, the transverse-field Ising model shows a paramagnetic phase where the spins have a preferred alignment in the direction of the applied magnetic field. That corresponds in a topological phase for the Majorana chain, showing two Majorana zero modes at the edges of the chain, as represented in Figure 1.1. When $\frac{\mu}{2t} = 1$, the system undergoes a quantum phase transition. These transitions are characterized by a scale invariance of many of the system properties, and they involve a lot of very interesting physics.

Majorana zero modes can be categorized as so-called non-abelian anyons, which means that exchanging two of these identical particles produces a change in the global quantum state of the system. This property could be used to store quantum information with a certain degree protection against local perturbations, because it depends on the relative location of the two tips of the nanowires and would not be affected by small local perturbations on any one of the tips. Taking advantage of this, they could potentially be used to construct qubits, and therefore, quantum computers in a potentially much more scalable way than other implementations [7].

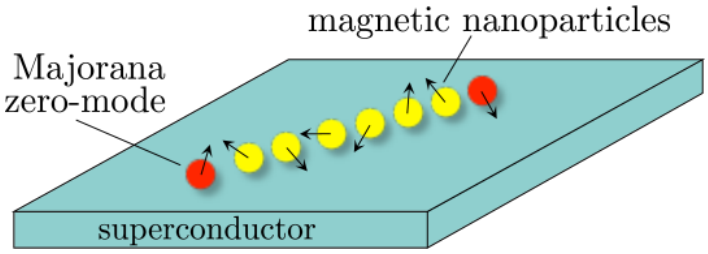

Figure 1.1: Representation of Majorana zero modes

Semiconducting nanowires can be used to experimentally implement the Majorana chain as seen in (1.1). In order to introduce the Δ and μ terms, the nanowires must be placed on top of an s-wave superconductor and under the influence of a magnetic Zeeman field [8]. The Majorana zero modes could be experimentally detected by measuring the electric conductance at the tips of the wires. It is expected that the observation of a quantization of the conductivity at certain particular values would be a strong signal for the existence of zero modes at the system. However this is hard to do in practice because, among many other factors, often disorder effects produce similar results and they are hard to eliminate[9].

It has been recently theorized that Majorana zero modes may not be enough for the development of a fully-functioning quantum computer. Nevertheless, there are generalizations of the Majorana chain that would give place to analogous quasiparticles which would allow a universal quantum computer [10]. The search for Majorana zero modes is, to date, a very active field of research, and so far there is no undisputed evidence of their observation.

1.3 Nanowire growth techniques

In general, complex structures in the atomic scale such as nanowires do not develop naturally and must be grown in a laboratory. The most common way to grow them is the liquid-vapour-solid method, where they develop stemming from the nucleation of semiconductor atoms in vapour phase into a solid , crystalline structure. This process is usually very slow, and to accelerate it a catalyst material in liquid phase, usually a gold droplet, is introduced to provide an interface for the nucleation of the material as represented in Figure 1.2. This allows for the atoms to adsorb to the droplet and nucleate into the solid phase through the interface at a much faster rate.

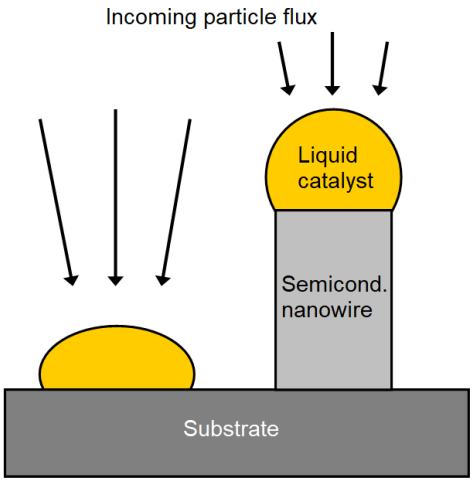

Figure 1.2: Representation of the vapour-liquid-solid method

This procedure may present some practical limitations when the grown nanowires have to be separated from their original substrate and deposited in another. This is because they have to be cut, transported to the desired location and then carefully laid down in place (such as implementing the Majorana chain). There is another growth procedure which could be potentially more scalable for these kind of applications called selective area epitaxy, where nanowires are grown directly on a substrate on which a semiconductor particle influx is applied. In this method, the substrate is covered by a dielectric mask where the material cannot grow, and a set of trenches are etched on the mask exposing the substrate with the desired geometry as represented in Figures 1.3 and 1.4.

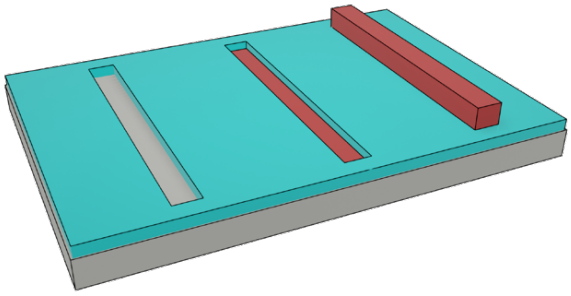

Figure 1.3: Representation of selective area epitaxy

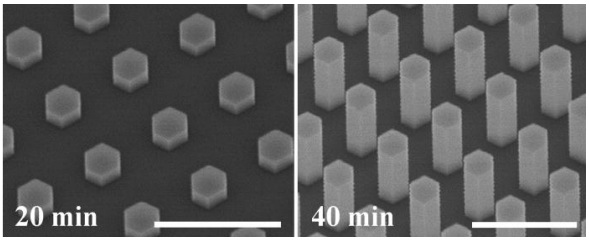

Figure 1.4: Implementation of selective area epitaxy [11] for hexagonal trenches

There are several experimental implementations for selective area epitaxy, depending on how the semiconductor material is applied over the surface. The first one is molecular

beam epitaxy (MBE), where a beam of semiconductor atoms is projected onto the surface by heating up a source in an extreme-vacuum environment. The vacuum is needed to avoid the deposition of impurities and to increase the mean free path of the atoms, however it is often very hard to achieve and makes the implementation impractical.
A second implementation is called metalorganic vapour-phase epitaxy (MOVPE), where the substrate is exposed to a vapour phase of the semiconducting material together with some organic precursor. The precursor is needed in order to have the semiconductor material in vapour phase, since usually it does not have the necessary chemical properties to reach it at reasonable temperatures. In this case, the vacuum is no longer needed and the environment can be set at moderate pressures, however the amount of impurities deposited onto the surface and the crystal increases substantially with respect to MBE. This method is widely used in industry, not only for the growth of nanowire but mostly for optoelectronic applications.

For the purposes of this work and regarding the model of nanowire growth, we do not need to worry about the particular experimental implementation of selective area epitaxy, but instead just consider its main elements in order to incorporate them into the model.

1.4 Experimental observations

Interestingly, three different growth regimes have been observed when growing certain semiconducting nanowires by selective area epitaxy [12]. These regimes are best observed when employing a rectilinear trench pattern, and are characterized by a difference in the growth rates of the different nanowires depending on their relative position with each other as represented in Figure 1.5.

The first one is the independent regime, where the nanowires grow independently with respect to one another, meaning there is no noticeable sharing of material between them or it is small enough to be disregarded. This can happen for example if the nanowires are sufficiently separated with one another.The second one is the competitive regime, where the nanowires located on the outer part of the pattern grow faster than those on the middle. An expected cause for this behaviour is that, in addition to the material coming from outside of the system, they capture material from the mask and they compete with each other for it. Then, since the nanowires on the outside of the pattern are exposed to a larger mask area and therefore to a greater amount of diffusing material, they grow faster than those in the middle. Lastly, the third of these is the synergetic regime, where the nanowires are believed to share material between each other by losing it to the mask. In this regime, the nanowires at the middle grow faster than those at the outer part, as they are exposed to a larger number of neighbours sharing material to the mask and leading to less losses.

These different regimes may open a window to better understand the mechanisms that govern the growth processes, because the former are macroscopic and observable while the latter are much harder to address experimentally.

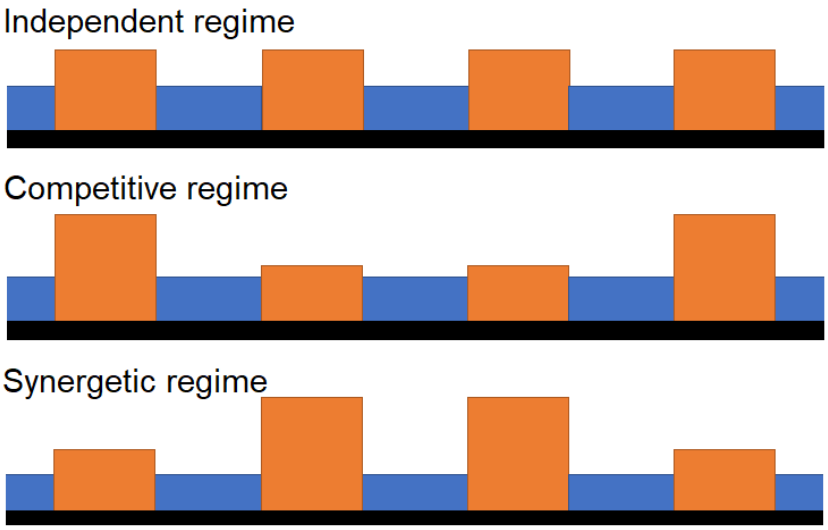

Figure 1.5: Representation of SAE growth regimes

1.5 Aim of this work

The objective of this work is to propose a simple model for the growth of semiconducting nanowires under the selective area epitaxy scheme, and to then solve it in order to explain its underlying growth mechanisms. Hopefully, the model can capture some properties of a real process, and therefore this understanding can contribute to shedding some light on the real growth mechanisms. This may provide more control in processes such as, for example, when fine-tuning the different experimental parameters (temperature, geometry, etc.) in order to optimize a growth process.

The model proposed is based on a set of microscopic, physically meaningful parameters. These parameters are not connected to experiment, but solving the model provides an experimentally observable window into these parameters in the form of a given growth regime. By observing this regimes for different combinations of the model parameters, we can try to come up with an explanation for their origin and thus the underlying mechanisms. Unfortunately, due to the theoretical nature of the parameters used, there are no sources in the literature that study them for this particular process and therefore it is not possible to fit the model more precisely.

An interesting, last step would be to relate the model to experiment by fitting the values of the microscopic parameters to those that match its solution to the experimentally observed results. This would enable to find out to what extent the model fits the real measurements and which generalizations or corrections are needed.

2 Methods

In order to come up with a model that describes nanowire growth, it is first necessary to intuitively understand the factors that influence selective area epitaxy. This is what will be done in this section to then present a model and the details of its numerical implementation.

2.1 Problem description

When modelling the growth of a nanowire array by selective area epitaxy, we should focus on capturing the different elements present. It is likely, however, that there are second-order corrections coming, from example, from the experimental implementation (MBE or MOVPE), or from many other causes, which could be subsequently addressed.

We have distinguished four different elements for selective area epitaxy as seen in Figure 2.1. The first of these elements is the effective incoming particle flux onto the system, described by a parameter G. It specifies the rate of adsorption of semiconducting atoms onto the surface. These adsorbed atoms, from now on called adatoms, diffuse randomly until they are either nucleated into the semiconductor crystal in the trenches or evaporated back to the vapour phase (or to the vacuum in the case of MBE). Note that not all of the incoming atoms $\tilde{G}$ adsorb to the surface, but only an effective portion $G = \tilde{G} \cdot p_s$ characterized by a sticking probability p_s. The second element is characterized by a diffusion constant D, representing the random motion of the adatoms within the surface. These adatoms will diffuse from the regions with a greater concentration to the regions with lower concentrations. The third element is characterized by an evaporation probability E, representing those adatoms that dissociate from the surface and return to the vapour phase. Then, finally the fourth and last element is given by a nucleation probability F for the adatoms to nucleate into the semiconductor crystal in the trenches.

The second element regarding diffusion is important in order to describe the sharing of adatoms between the mask and the nanowires. Classically, it is described by two equations called the Fick laws,

$$J = -D \cdot \nabla c \qquad \text{First Fick law,} \tag{2.1}$$

$$\frac{\partial c}{\partial t} = \nabla (D \cdot \nabla c) \qquad \text{Second Fick law.} \tag{2.2}$$

The first law states that the flow of matter is against the concentration gradient, proportionally to a diffusion constant D. The second law is just a continuity equation for the diffusing particle density, c.

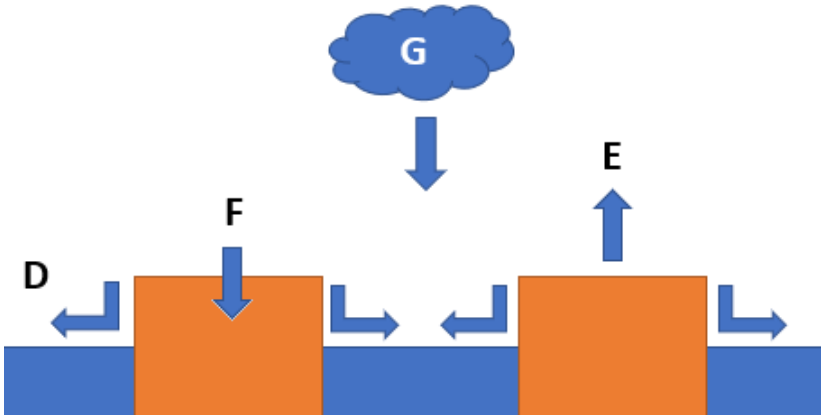

Figure 2.1: Representation of the SAE components

We only need the second law to characterize diffusion. If sufficient time is allowed to pass after the incoming flux of particles is turned on, then the particle concentrations will equilibrate much faster than the growth occurs and we can consider the diffusing particle density c to be independent of time. Then, using this approximation the dynamics reduce to the steady-state form of the second Fick law:

$$\nabla(D \cdot \nabla c) = 0 \qquad \text{Steady-state second Fick law} \tag{2.3}$$

Even though it has not been previously included, temperature is another fundamental element in selective area epitaxy. However, it is rather complicated to model.
A simple way to introduce temperature in chemical processes is through the Arrhenius law. Given a parameter of the system A, with an associated activation energy E_A and the Boltzmann constant k_B, the Arrhenius law models the effects at a temperature T as

$$A \rightarrow A(T) = A \cdot \exp\left(-\frac{E_A}{k_B T}\right). \tag{2.4}$$

This equation is considered to be a simple empirical relation, however, it works relatively well in some cases such as for diffusion processes. The Arrhenius factor makes the given parameter A effectively diminishes the value of A and makes it converge to zero with the temperature, as shown in Figure 2.2, and to converge to its original value as $T \rightarrow \infty$. We can find in the literature how the diffusion constant D fits approximately well the Arrhenius law for selective area epitaxy [13]. The resulting activation energy for the self-diffusivity is on the order of kcal/mol ($\approx 5 \cdot 10^{-2}$ eV)[14].

Trying to model the effects of temperature on parameters other than the diffusivity, such as nucleation, evaporation and sticking probabilities can be problematic, as it is not known to what extent it is justified to use the Arrhenius law. Moreover, this law introduces many additional parameters in the form of activation energies with unknown empirical values, increasing notably the degrees of freedom of the model, and therefore its complexity. For these reasons, unfortunately the temperature was finally not included in this work's model, despite its relevance.

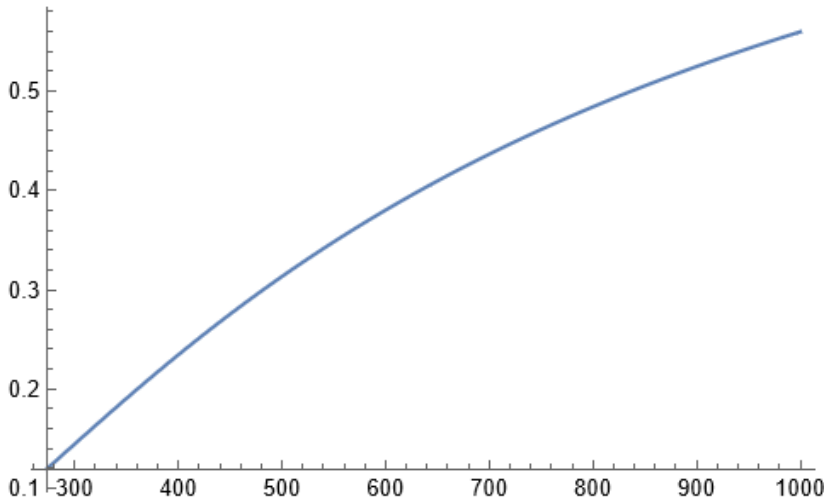

Figure 2.2: Plot of the Arrhenius factor $\exp\left(\frac{-E_A}{k_B T}\right)$ for $E_A = 0.05$eV and T between 273 and 1000 Kelvin

2.2 Research approach

At the beginning of this work, two models were considered in order to implement the elements shown in Figure 2.1. The first one consisted in an stochastic process where the path of each adatom was modelled as a random walk. The parameters of the model would represent the probabilities of the particles to adsorb to the substrate, nucleate into the crystal or evaporate back to the vapour phase as seen in Figure (2.1). The second model consisted in a diffusion process described by a two-dimensional partial differential equation, with parameters also describing the aforementioned probabilities. Both models should be in principle equivalent, as long as a relationship between their parameters is found.

However, the model chosen in the end is a differential equation built upon the second Fick law instead of the stochastic process. This model allows us to introduce diffusion in a more natural way through the diffusivity D, as well as to find the steady-state solution directly. This is more advantageous than compared to the stochastic process, which only allows for the adsorption of a limited number of particles and is less computationally efficient. On the other hand, the stochastic process allows for the observation of the time evolution of the system, which could be useful when the steady-state approximation is no longer reasonable.

Derivation of the differential equation

The first thing to do is to derive the differential equation for a selective area epitaxy process, capturing the components shown in Figure (2.1). We use as a starting point the second Wick law in its steady-state form (2.3). Then, we introduce the effective particle flux G as a source term, and the nucleation and evaporation probabilities E and F as a sink term (effectively removing adatoms from the surface), resulting in the following equation:

$$\nabla(D \cdot \nabla c) - (E + F) \cdot c + G = 0. \tag{2.5}$$

The nucleation and evaporation probabilities act as a sink term proportionally to the

density of adatoms c. Each of the parameters in the equation take two values as a function of the position on the surface, depending on whether they describe the trenches or the mask.

An equivalent, but more physically meaningful formulation comes from considering the characteristic times and lengths of the adatoms. The diffusion constant D depends on these two parameters [15] as:

$$D = \frac{L^2}{4t}. \tag{2.6}$$

The characteristic time t describes the average time during which a diffusing adatom stays in the surface until it disappears, either because of nucleation or evaporation, and the characteristic length L describes the average displacement of that diffusing particle during time t. Then, using the definition of the characteristic time, we can replace the evaporation and nucleation probabilities as

$$E + F = \frac{1}{t} = \frac{1}{t_E} + \frac{1}{t_F} \tag{2.7}$$

which allow us to decompose the differential equation in terms of these two parameters, becoming

$$\nabla\left(\frac{L^2}{4t}\cdot\nabla c\right) - \frac{c}{t} + G = 0. \tag{2.8}$$

Note how there is an ambiguity about how the adatoms are removed from the surface, either from evaporation or nucleation into the crystal, allowing us to reduce the number of parameters from four to three.

Another possible way to express this equation would be in terms of the planar growth rates $g_p = \frac{c_p}{t_F}$ of the nanowires on the mask and the substrate by solving for the planar concentration $c_p = G\cdot t$. The equation would take the form

$$\nabla\left(\frac{L^2}{4t_F}\frac{G}{g_p}\cdot\nabla c\right) + G\left(1 - \frac{c}{g_p t_F}\right) = 0. \tag{2.9}$$

This form could be more useful when trying to implement temperature, as the planar growth rate is better connected to experiment than the characteristic time and lengths. However, note how it is also necessary to include the characteristic nucleation time of the adatoms t_F in each region, that is, the average time an adatom lasts before nucleating disregarding evaporation. Because of this, the formulation seems slightly more impractical than (2.8).

Using characteristic times and lengths, while physically meaningful, poses some problems because they have little connection to experimental observables and their values are hard to observe. This means that it is difficult to set their numerical values in the model, and also they are hard to find in the literature. Due to this, we expect to obtain qualitative information about the growth regimes by considering the ratios of the values between the mask and the trenches, and sampling over an ample range of them.
Using the ratios between the values of the parameters at the mask and the trenches is justified if the effect they produce on the growth regime depends on the relative strengths on those regions. If, on the other hand, their effect does not depend on the relative strengths, it makes more sense to use their absolute value.

Solving the diffusion equation

The second step is to solve the proposed differential equation (2.8). We believe that it is hard to approach it analytically due to the dependence of the parameters on the geometry of the domain, so it should be solved numerically. However, for certain geometries the equation reduces to an ordinary differential equation in one dimension which could be more easily approached. This is the case for the rectilinear trench geometry used together with periodic boundary conditions, where the equation (2.8) reduces to

$$\frac{\partial}{\partial x}\left(D \cdot \frac{\partial c(x)}{\partial x}\right) + (E+F) \cdot c(x) + G = 0. \tag{2.10}$$

The parameters would become step functions in the form

$$D(x) = \begin{cases} D_{trench} & x \in \Omega_{trench} \\ D_{mask} & x \in \Omega_{mask} \end{cases} \tag{2.11}$$

where Ω is the domain of the differential equation. However, we have kept the general method by solving the whole partial differential equation in order to allow for the use of an arbitrary geometry and more complex boundary conditions.

There are many differential equation solvers available, and the one chosen for this model is the so-called finite-element method which solves the equation by discretizing it on a mesh of triangular elements with a given average size. As long as the method converges, we can increase the accuracy of the solution to arbitrarily high values by increasing the number of triangular mesh elements for each spatial dimension.
The implementation has been performed in Python using a library called FEniCS, which is a popular and open source automatic finite-element solver [16].

To solve the equation we need to choose the boundary conditions for the domain. In order to remove the influence of the boundary on the solution, we have chosen periodic boundary conditions, which imply an infinitely repeating trench pattern. For a rectilinear-trench geometry as seen in Figure (2.3), these boundary conditions effectively set infinitely long nanowires in the y-direction, and an infinitely repeating pattern in the x-direction. Other possibilities are open boundary conditions, setting either the concentration or the flux of adatoms at the boundary.

2.3 Experimental setting

In order to solve the equation, the geometry of the trenches must be specified, and also the parameters d, t, L and G must be set to some numerical values.

The domain used to represent the mask is chosen to be rectangular with dimensions $L_x = 300$ and $L_y = 100$. The units for these dimensions (for example, nanometres) also determine the length units of the rest of the parameters such as the characteristic length or the diffusion constant. However for this work they remain unset.
The x-dimension is set larger in order to allow for more separation between the trenches, which will be useful when the trench separation is increased in order to avoid an overflow. The domain then presents 5 rectilinear trenches, each with a width $w_x = 10$ and a variable separation d between them.

The rectilinear trench geometry is useful in order to easily project the adatom density onto the x-direction perpendicular to the trenches, and in this way observe the shape of the nanowires in a single dimension. This makes it easier to observe the different growth regimes, even though it is expected that they should also be present in an arbitrary geometry.
The accuracy of the model is given by number of mesh elements m which is set to be more dense in the perpendicular x-direction because that is where the adatom concentration c changes the most in a rectilinear trench geometry with periodic boundary conditions. As mentioned before, for periodic boundary conditions the differential equation (2.8) effectively reduces to an ODE so that we can use the values of $m_x = 300$ and $m_y = 1$, ignoring the y-direction parallel to the nanowires. This would not be the case if other geometries or other boundary conditions were used, due to boundary effects.

The parameters in the mask are set with the arbitrary values of $(t, L, G)_{mask} = (10, 10, 10)$. The values for $(t, L, G)_{trench}$, as well as the separation d between the trenches will be set from an evenly spaced range.

Solutions to the diffusion equation showing synergy

After numerically solving the diffusion equation (2.8), the steady-state distribution of adatoms across the surface is obtained allowing us to explore the shape of the nanowires by projecting the distribution onto their transverse direction. This profile provides information about the adatom density in the mask and the trenches.

For example, for a system with parameters $(d, t, L, G)_{trench} = (50, 40, 50, 1)$ and $(d, t, L, G)_{mask} = (10, 40, 10, 0)$ chosen in purpose to obtain a strong synergetic regime, we obtain a solution as seen in the figures (2.3), (2.4) and (2.5).

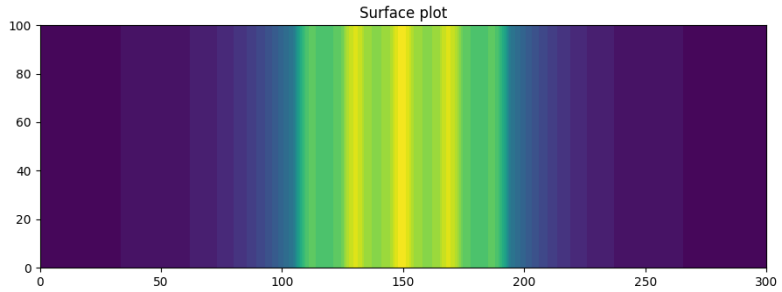

Figure 2.3: Surface distribution of adatoms

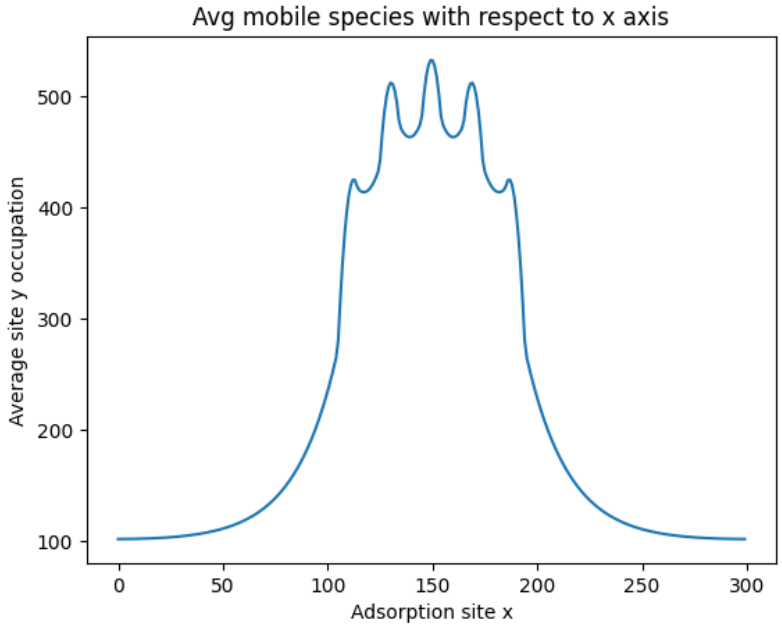

Figure 2.4: Adatom density perpendicular to the trenches for a synergetic regime

Instead of the adatom density, the nanowire growth rates can be computed by introducing the nucleation rate F which was not needed to solve the equation. The growth rate can be computed by just multiplying element-wise the density of adatoms in the trenches seen in Figure (2.4) by F_{trench}, and the density in the mask by F_{mask}. Usually, the growth rate in the mask will be zero, $F^{mask} = 0$ because the nanowires are expected to grow only on the substrate. One thing to consider is that the related characteristic nucleation time, $t_F = F^{-1}$ should be larger than the overall characteristic time t because an adatom that can only nucleate will last more than an adatom that can both nucleate and evaporate. The resulting growth rates can be observed in Figure (2.5)

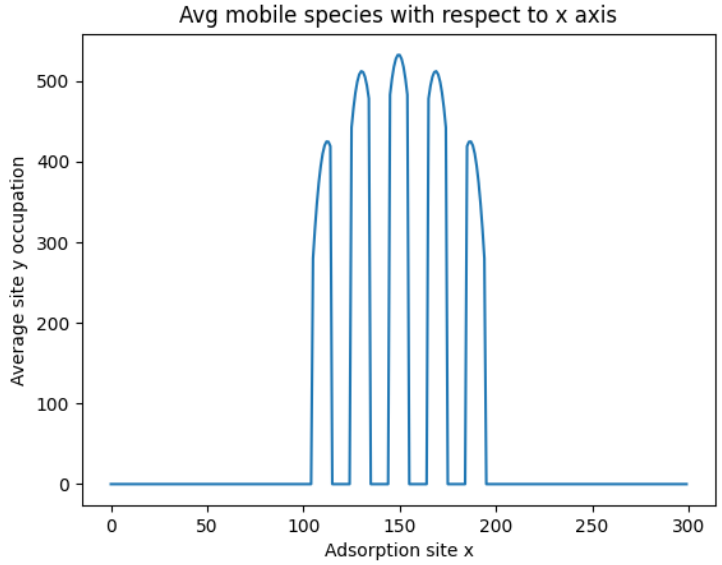

Figure 2.5: Nanowire growth rate for a synergetic regime

The growth rate could be easily related to experiment by comparing the observed

nanowire heighs to the growth rate multiplied by the exposition time of the trenches to the incoming particles.

Solutions to the diffusion equation showing competitiveness

If we modify the parameters, we can instead obtain a competitive regime. This regime is fundamentally different from the synergetic one because the density of adatoms in the trenches is lower than the density in the masks, allowing for a net flux of adatoms from the mask into the trenches, and a characteristic convex shape as can be seen in Figures (2.6) and (2.7).

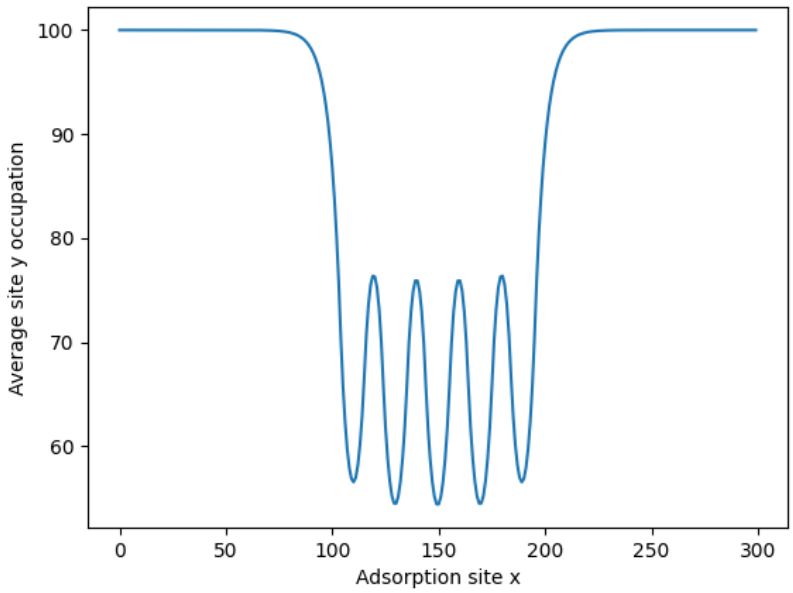

Figure 2.6: Adatom density perpendicular to the trenches for a competitive regime

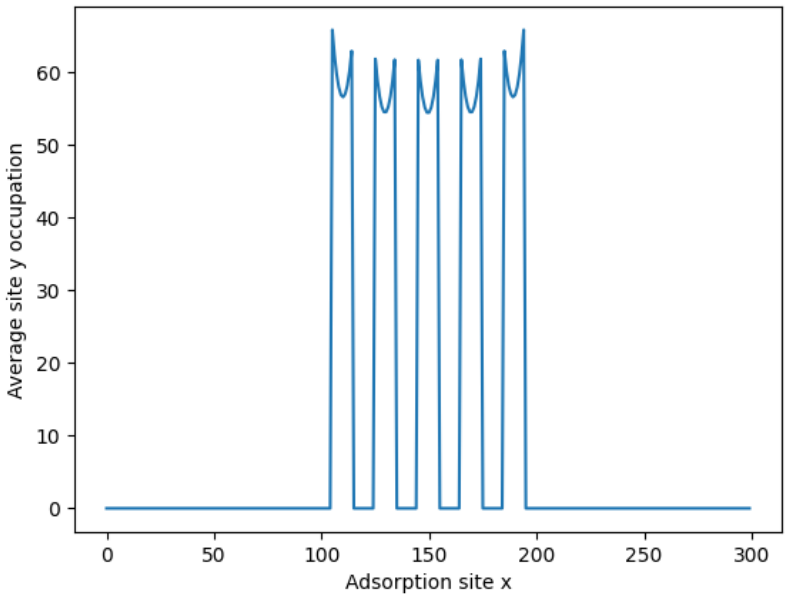

Figure 2.7: Nanowire growth rate for a competitive regime

Solutions to the diffusion equation for an arbitrary geometry

The method used to solve the differential equation (2.8) is indifferent to the underlying trench geometry, so it becomes very simple to solve it for an arbitrary geometry such as in Figure (2.8). Nevertheless, it is more convenient to stick to rectilinear trenches in order to be available to observe the different growth regimes by only projecting onto the perpendicular dimension. However it may be interesting to observe the effects of the different growth parameters in more complicated geometries.

For example, it may be possible to observe the effects of synergy in two directions by means of an hexagonal pillar geometry, where the amount of synergy that a certain pillar experiences would be proportional to the number of neighbours that it has. This could be approached computationally with a model like this to, for example, compare with experiment and check if the model captures the real behaviour. Also, it could be used as an alternative way to calibrate the model parameters.

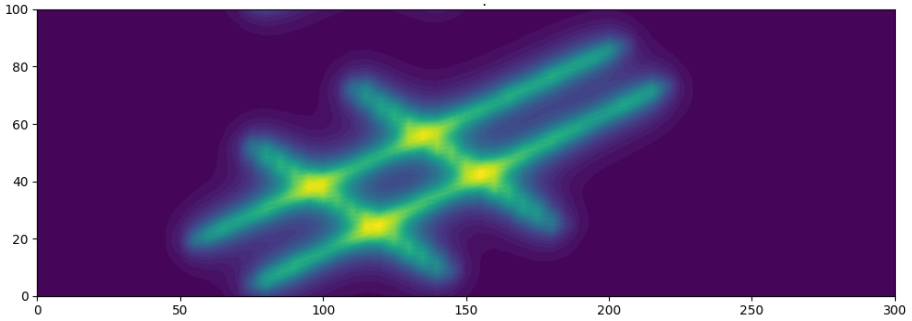

Figure 2.8: Distribution of adatoms for a hashtag geometry

Exploration of the growth regimes as a function of the parameters

In order to explore the growth regimes, it is useful to study the difference in height between the trench on the outside of the pattern and the trench in the middle. This height difference can be used as a macroscopic observable r to distinguish between the different regimes depending on the numerical parameters used. The difference in the areas under the curve of the average adatom distribution, such as the one seen in Figure (2.4) can also be used as an observable for the same purposes. In all cases, if the magnitude $r = r_1 - r_0$ is positive, it means that the regime is synergetic since the height or area of the inner trench r_1 is greater than the outer one r_0. Otherwise, if r is negative the regime will be competitive. If $r = 0$, the regime is independent and the nanowires grow at the same rate. It is expected for this magnitude to depend on the trench spacing d and to become zero for large d.

By solving the differential equation several times varying the values of (d, t, L, G) in the trenches from a given range, we can obtain a set of plots of the observable r given by the relative height difference between the innermost and outermost wires, and that can hopefully show us some qualitative information about the different growth regimes.

3 Results

In this section the results corresponding to the solution of the differential equation (2.8) are shown, which shed light on the role of the parameters on the model and allow us to obtain qualitative information about the different growth regimes. However, before doing this it is important to argue why, for some of the parameters, it is justified to employ the ratios between the mask and the trenches instead of their absolute value. In order not to slow down the exposition, this is shown in the appendix, where we learn that employing the ratios makes sense for the characteristic time t as well as the input flux G, while it does not for the characteristic length L and the nanowire separation d. The reason is that for the first two parameters, their largest contribution comes from the relative strengths between the trenches and the mask. However, for the second two this is no longer the case and their largest contribution comes from their absolute value instead. What is done instead is to set $L_{trench} = L_{mask}$ and vary it together with d from a given range of values.

Below, we see the results after solving equation (2.8) for different values of the parameters. The plots show the evolution of the observable r given by the height difference of the inner and outermost nanowires after varying the different parameters. Since the model presents four free parameters, two of them must be fixed in order to plot the other two. We have to choose a particular value to fix the parameters, noting that it adds a bias to the results. However, we believe that the following figures captures well enough the overall behaviour of the model in spite of this bias.

3.1 Fixed separation and input flux

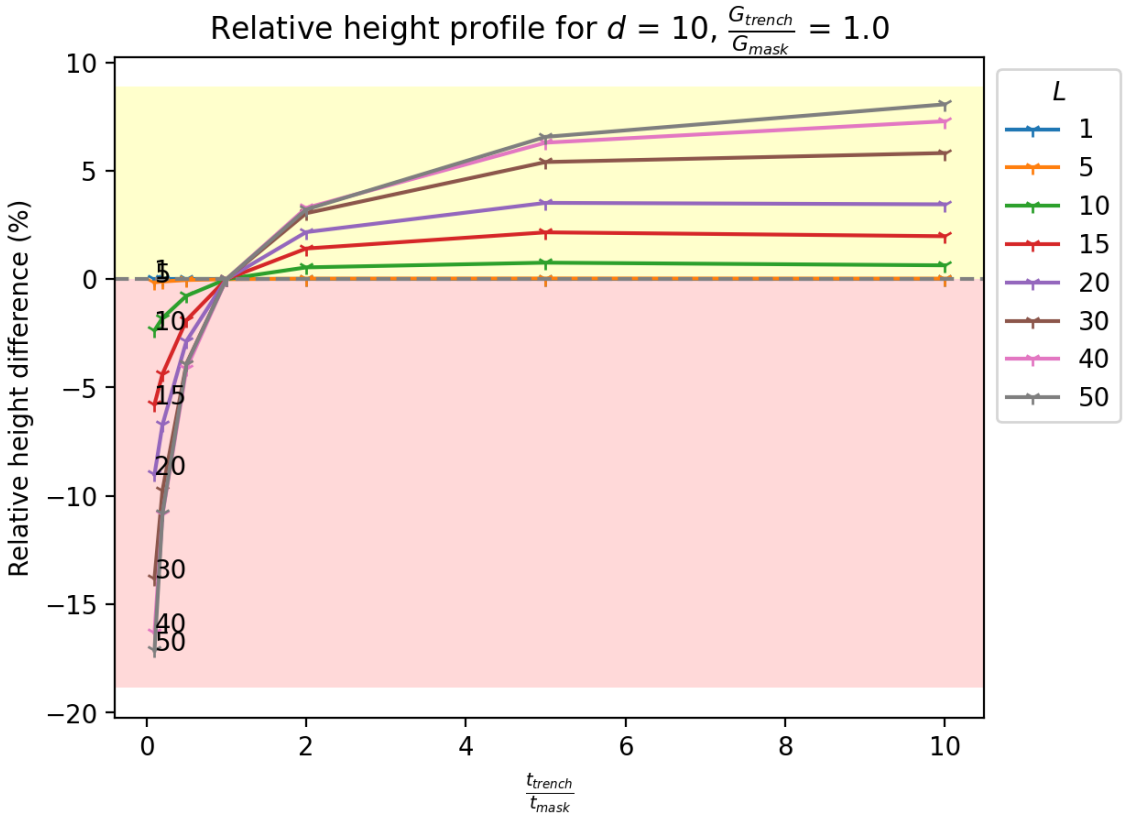

Figure 3.1: Results after fixing the nanowire separation and the input flux

Figure (3.1) shows the behaviour of the observable after fixing the separation between the nanowires with a value $d = 10$ (having a nanowire width of $w_x = 10$), as well as fixing the influx of particles in the trench equal to that in the mask. The free parameters are then the ratios between the characteristic times and the values for the characteristic lengths $L = L_{trench} = L_{mask}$. The yellow region corresponds with a synergetic solution while the red region with a competitive one.

It can be appreciated how increasing the value of the characteristic time in the trenches results in a higher synergy for all values L. This is logical if the characteristic time is interpreted as the average time the adatoms last in the surface. Thus, a longer characteristic time in the trenches equals a higher density of adatoms there and thus a greater amount of material they can potentially share with each other, meaning greater synergy.
On the other hand, when the characteristic time in the mask dominates, the opposite happens and a competitive regime is obtained. This may be explained by the fact that there is a higher density of adatoms in the mask and therefore the nanowires on the outside of the pattern, exposed to a larger mask area, are able to capture more material.

Simultaneously, increasing the value for the characteristic lengths boosts whichever regime the system presents, whether synergy or competitiveness. This is reasonable if the characteristic length is understood as the distance that the adatoms are able to travel before being removed from the surface. In other words, it defines how much material is

able to cross the boundaries between mask and trenches, therefore increasing synergy if the direction of the flux is from trench to mask, or competitiveness it the direction of the flux is from mask to trench.

Note how the inflection point between the different regimes takes place at the point $\frac{t_{trench}}{t_{mask}} = 1$ since there is no difference mask and trenches and the corresponding adatom concentration is uniform across te surface. Note also how for smaller values of L, the regime converges to independent as the trenches are not able to share almost any material with each other.

3.2 Fixed separation and characteristic length

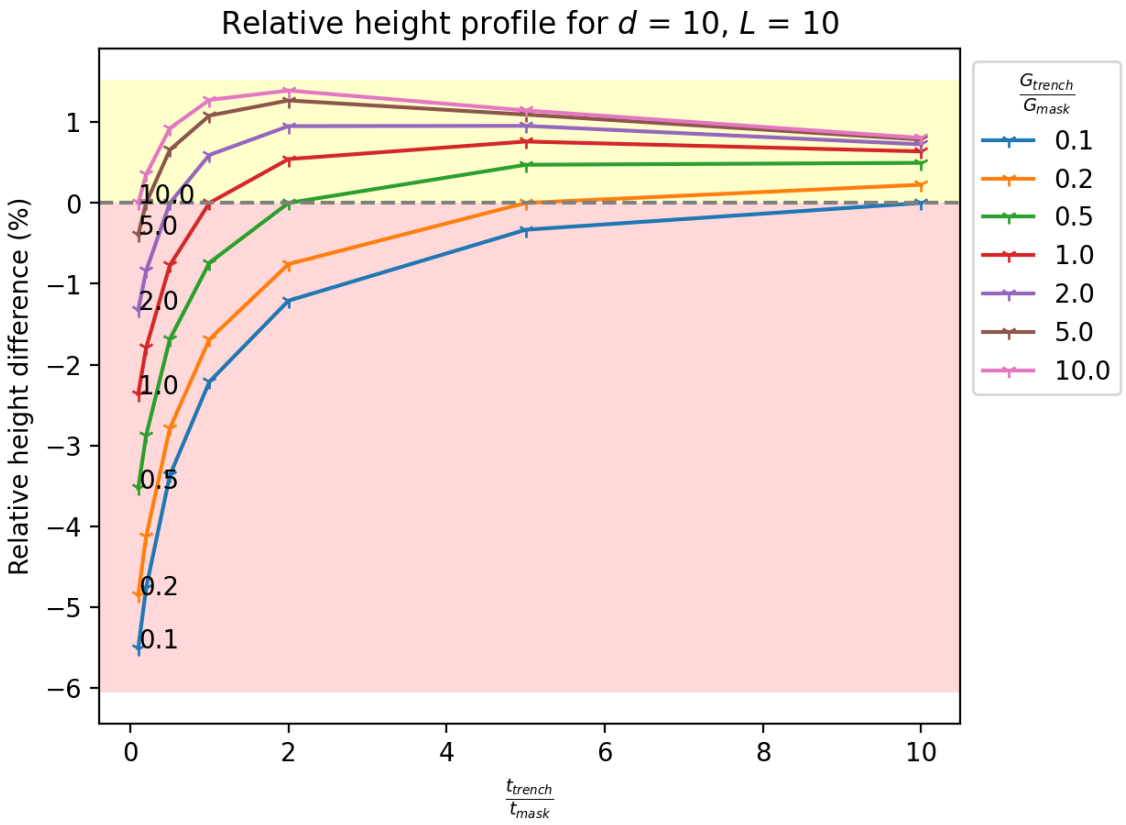

Figure 3.2: Results after fixing the nanowire separation and the characteristic length

In Figure 3.2, the behaviour of the observable can be seen after fixing the distance between the nanowires as well as the value of the characteristic lengths, leaving free the ratios between characteristic times and input fluxes.

It can be seen how the characteristic time in the trenches still produces the same effect: increasing the synergy in all cases. Simultaneously, the input flux in the trenches also increases synergy. This makes sense since the main factor for synergy is the density of adatoms in the trenches, and the input flux also contributes to increasing this density. In turn, if the input flux in the mask is higher, other things being equal, there is a higher density of adatoms in the mask and therefore the regime becomes competitive.

Note how there is an inflection point on the green line for $\frac{t_{trench}}{t_{mask}} = \frac{G_{trench}}{G_{mask}} = 1$, where height difference is equal to zero, while varying the ratios of t or G from that tipping point gives rise to synergy or competitiveness respectively.

Also note how there is a value for G_{trench} where the synergy is saturated, probably because for the given value of L, the trenches are not able to share more material among themselves and a bottleneck occurs. In effect, in Figure 3.3 it can be seen how by setting $L = 40$ a higher value for both synergy and competitiveness is obtained.

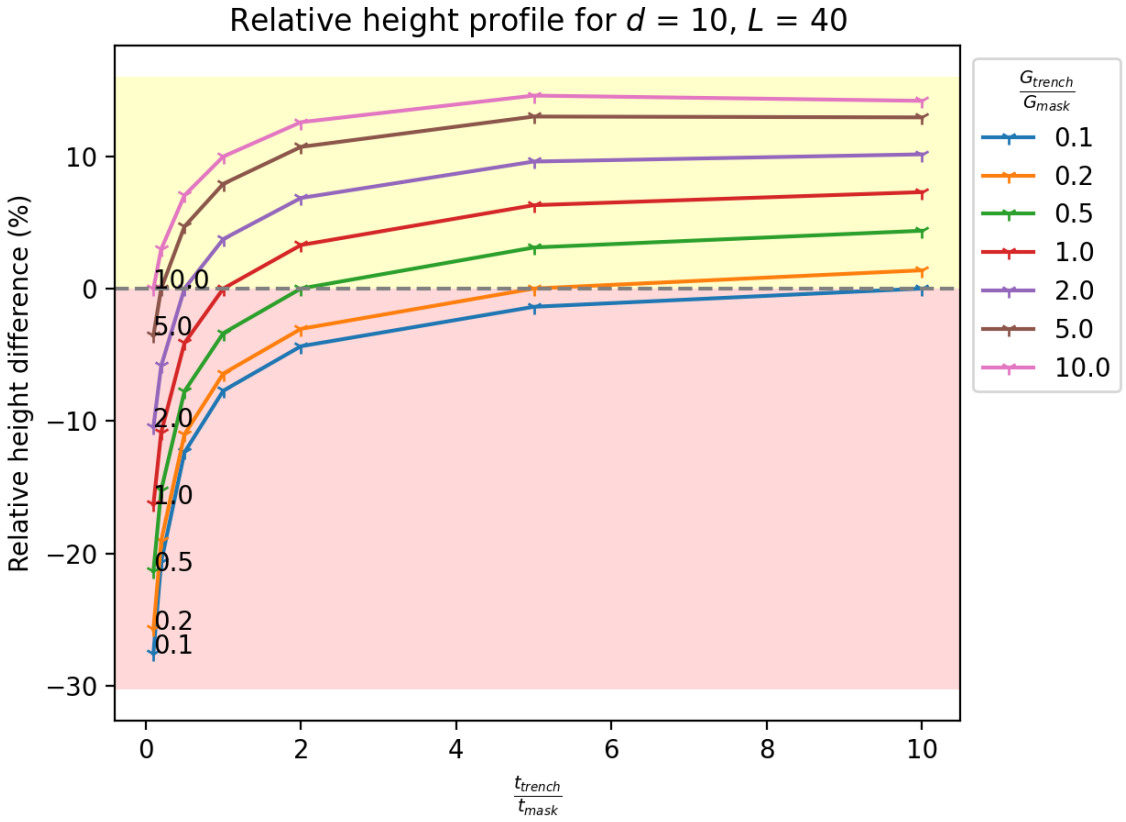

Figure 3.3: Results after fixing the nanowire separation and the characteristic length (larger characteristic length)

3.3 Fixed separation and characteristic time

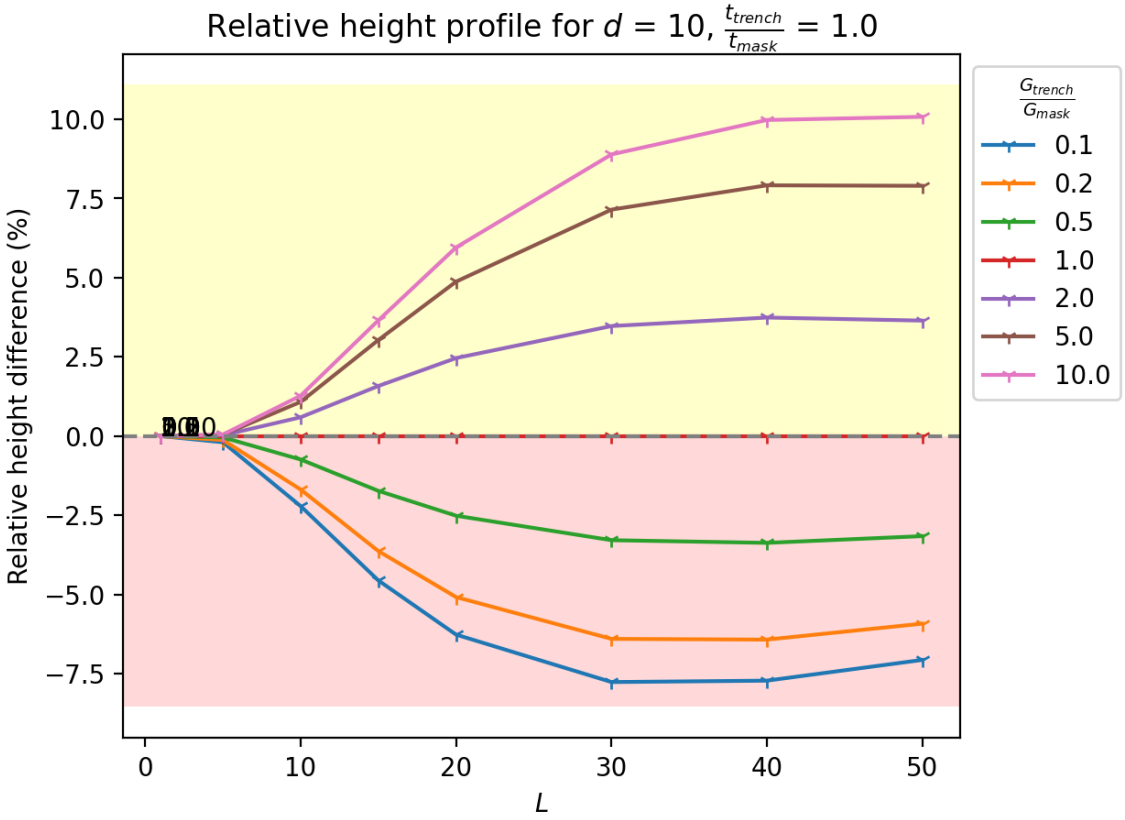

Figure 3.4: Results after fixing the nanowire separation and the characteristic time

In Figure 3.5, the behaviour of the solutions after fixing the separation between the nanowires as well as the ratio between the characteristic times can be observed. It can be seen how, if the input flux dominates in the trenches, synergy is obtained. On the other hand, there is competitiveness if it dominates in the mask. These effects are influenced by the value of the characteristic lengths as for in Figure (3.2).

Note how when also the ratio for the input flux is set to one, the independent regime is obtained since the density of adatoms is the same at both the mask and the trenches and the system is not able to distinguish between both regions. Also note how for the valus of L close to zero, an independent regime is obtained since the exchange of material between mask and trenches no longer occurs.

3.4 Fixed characteristic time and length

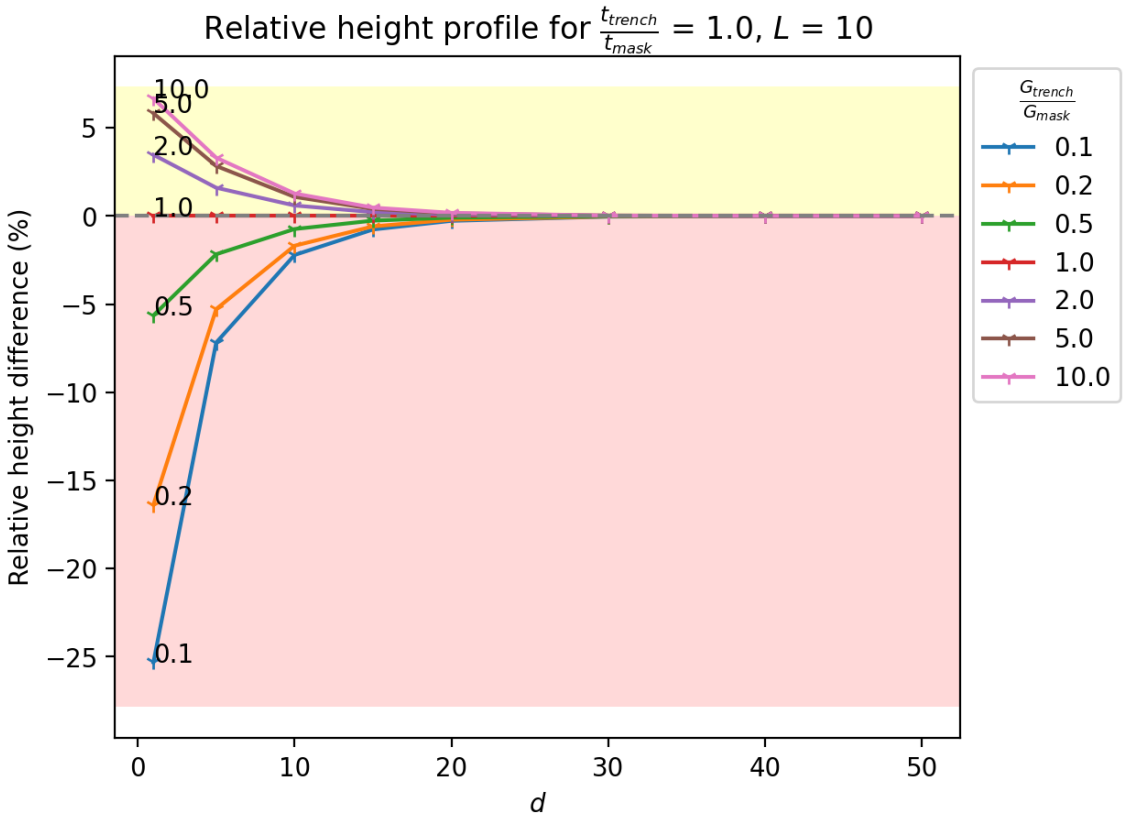

Figure 3.5: Observables fixing characteristic time and length

Next, in Figure 3.7, the behavior of the solutions can be seen after varying the distance between the nanowires and the ratios for the input flux, setting the ratios between the characteristic times and the values for the characteristic lengths. For a large separation between nanowires, the regime tends to become independent while it increases in intensity for either synergy or competitiveness for small separations, agreeing with the expected behaviour.

The input flux plays the same role as the characteristic time, increasing the density of adatomas at a region so that if it dominates in the trenches there is synergy, while if it dominates in the mask there is competitiveness.

3.5 Fixed characteristic time and input flux

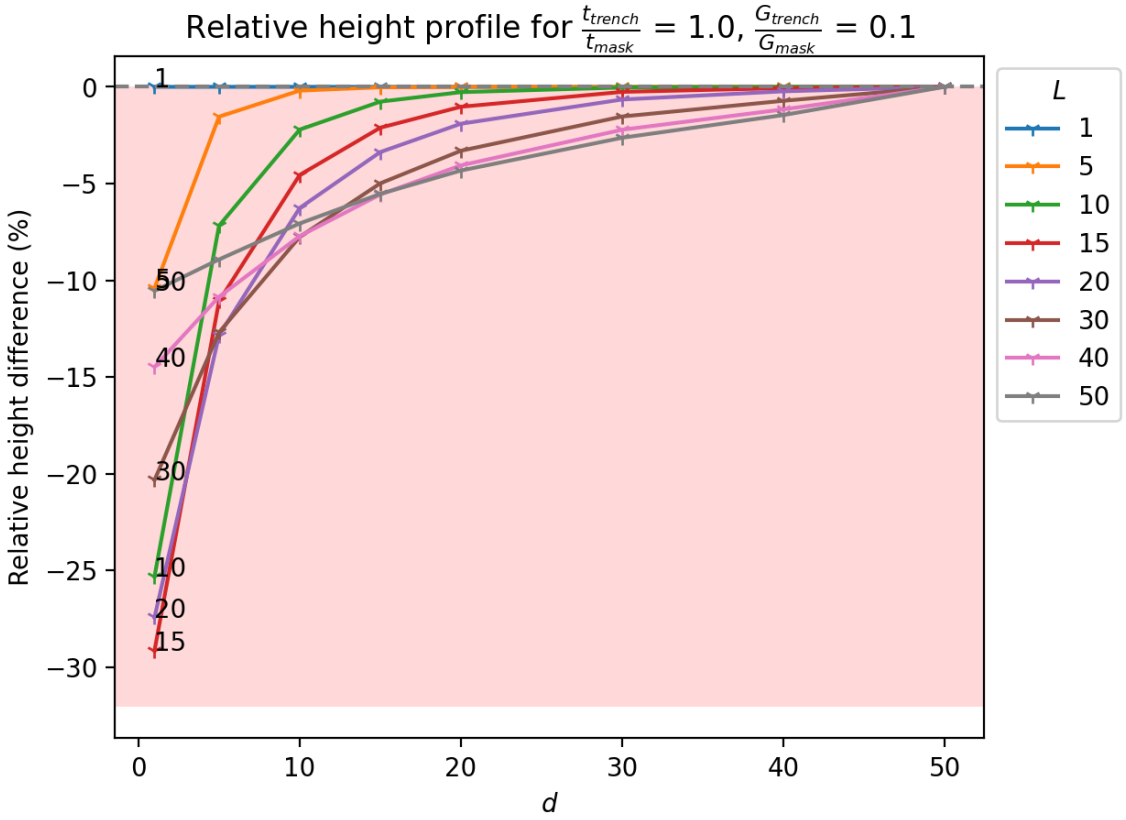

Figure 3.6: Observables fixing characteristic time and effective input flux

In Figure 3.6 we can see the solution fixing the characteristic times and the particle fluxes. The results are always either purely competitive or purely synergetic, reinforcing the fact that the characteristic lengths and nanowire separation do not influence which type of regime happens, only its intensity. The type of regime in this model is only characterized by the density of adatoms at each region, due to $\frac{t_{trench}}{t_{mask}}$ and $\frac{G_{trench}}{G_{mask}}$. This parameters can be balanced with each other, giving place to a uniform concentration across the surface, for example after setting $\frac{G_{trench}}{G_{mask}} = \frac{t_{trench}}{t_{mask}}$.

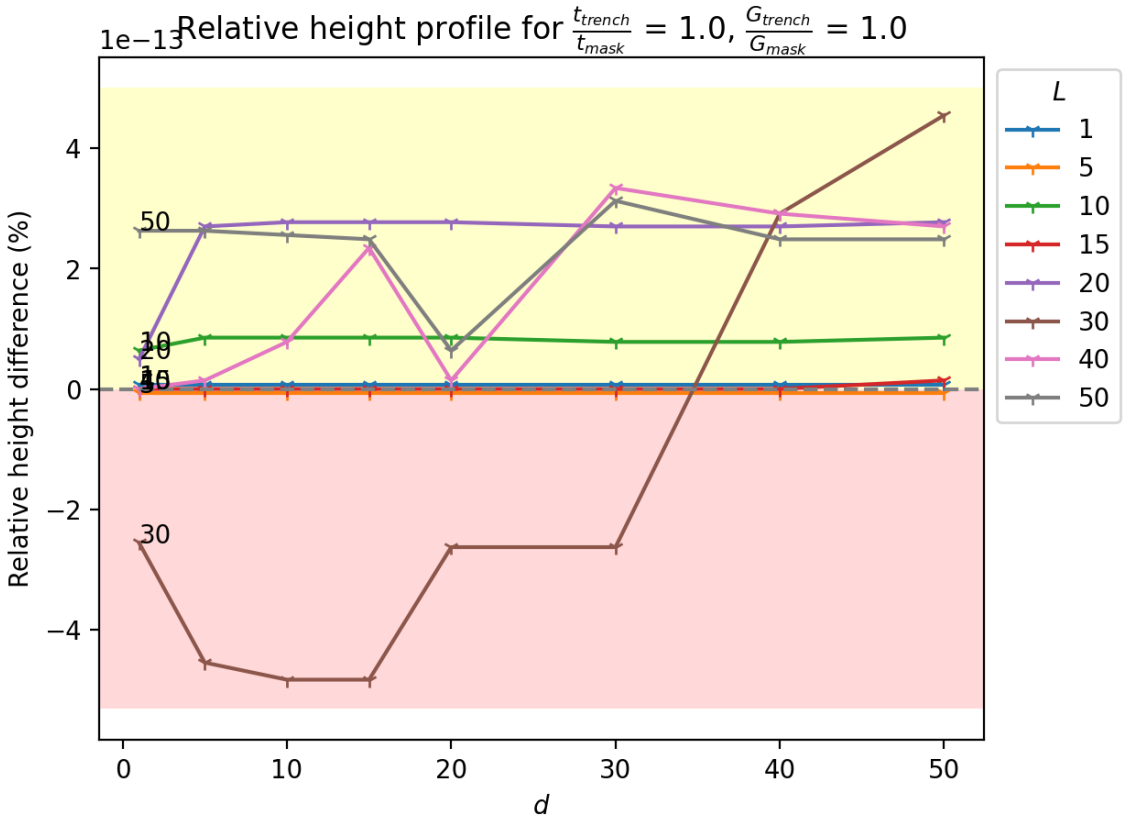

Figure 3.7: Observables fixing characteristic time and effective input flux

In Figure (3.7), the behaviour of the observable can be seen after setting the ratios for the characteristic times and input fluxes equal to one. By setting both to unity, the regime is independent for all values of L and d (observe that the height difference is multiplied by 10^{-13}), which was expected because the adatom density becomes uniform.

It is always possible to obtain a balance between t and G such that the resulting regime is independent. This relationship can be obtained by observing the value of $\frac{t_{trench}}{t_{mask}}$ at the point of intersection of Figure (3.1) with the x-axis, as a function of $\frac{G_{trench}}{G_{mask}}$. This balance can be understood as an equality in the densities of adatoms in the mask and trench, in the trenches because the adatoms survive longer and in the mask because more adatoms arrive per unit of time. Curiously enough, this balance occurs when $\frac{t_{trench}}{t_{mask}} \cdot \frac{G_{trench}}{G_{mask}} = 1$ regardless of their values.

3.6 Fixed characteristic length and input flux

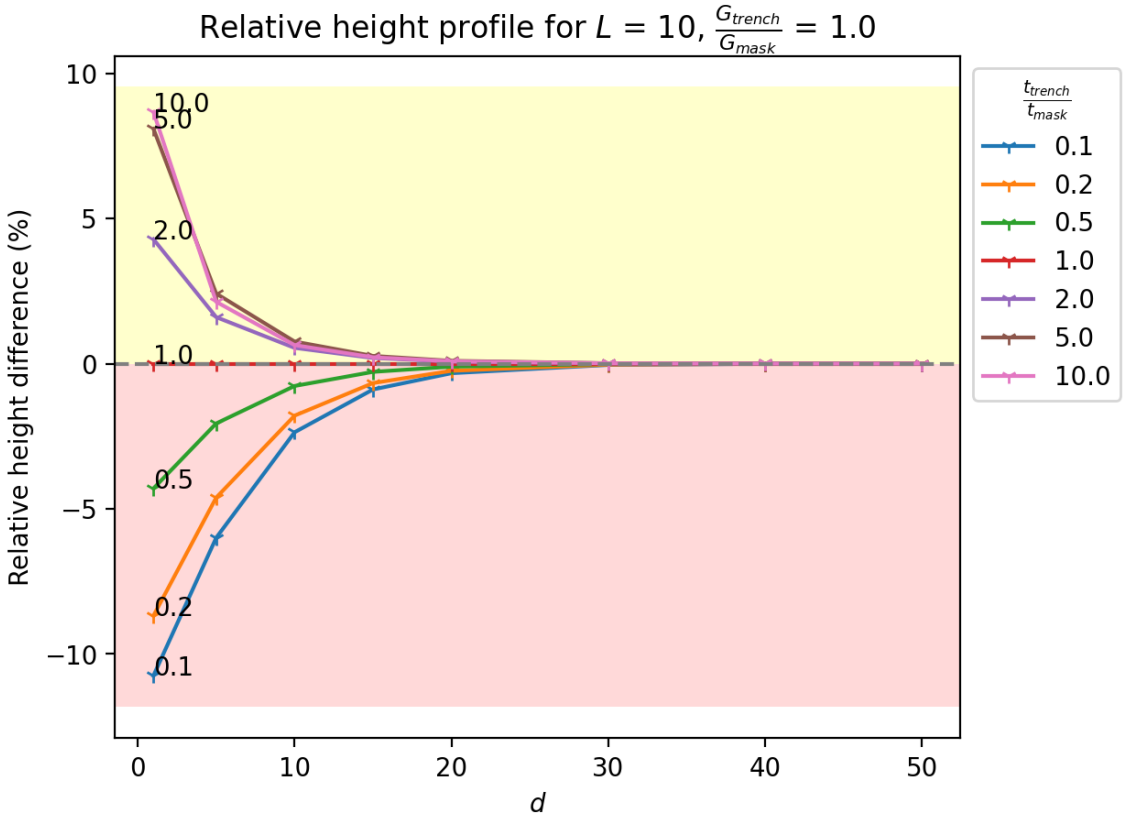

Figure 3.8: Observables fixing characteristic length and effective flux

Finally, in Figure (3.8), both the characteristic lengths and the ratios for the input fluxes are fixed and the expected behaviour is obtained. For large d, the independent regime is reached asymptotically. On the other hand, for small d a larger characteristic time ratio gives rise to higher synergy and a smaller characteristic time ratio gives rise to competitiveness.

4 Discussion

In the results above, the role played by each of the four parameters in the model has been hypothesized. This has allowed to get an intuitive picture of what the underlying mechanisms are for the growth of nanowires in this simple selective area epitaxy model. More particularly, that the appearance of the different regimes is supposed to be due, mostly, to the density of adatoms in the mask and trenches. If this density is greater in one region than in another, then there is an exchange of material between them due to diffusion which gives place to a difference in the heights of the nanowires.

The adatom flux between mask and trenches gives rise to synergy if the density of adatoms in the trenches is greater than in the mask, since then there is a net flux of material to the mask. Therefore, the nanowires on the outer parts of the pattern more material than those in the centre, giving rise to the characteristic synergy shape. The opposite happens if the density of adatoms in the mask is greater, because then there is a net flux from the mask and into the trenches and the outermost wires grow faster because they are exposed to more mask. Furthermore, the particle density in a region is characterized by two factors: the characteristic time of the adatoms on it and the amount of adatoms arriving per unit time, i.e., the effective input flux of material.

On the other hand, diffusion is mainly characterized by the characteristic length in the regions. At a higher value of L, more matter can escape from one region to reach the adjacent ones. This parameter plays an important role in amplifying the regimes, but it does not alter their type since they are mainly due to the difference in densities between the regions.

Finally, it has been observed how the distance between nanowires plays a role analogous to the characteristic length, amplifying or decreasing the intensity of the regimes. This is because decreasing the distance between trenches increases the relative effects produced by the diffusion of particles and also the other way around.

In short, the difference in height between peaks has been used as a useful observable to figure out this simple model. The question is whether this study could be generalized to more complicated models, which could represent more faithfully what happens in an experiment.

There are many elements that could be included or improved in future iterations of the approach. The first of them is temperature, which was left out and could be incorporated into the mode. For that, the use of Arrhenius law should be justified and the problem of adding many activation energies in the form of parameters should be addressed. One possible approach for this would to reformulate the differential equation in terms of the growth rate as seen in 2.9, which scales with the Arrhenius law, and thus be able to explore values found in the literature for the growth rate activation energy for some semiconducting nanowires, such as in [17].

On the other hand, it may be interesting to explore an analytical treatment of the differential equation (2.8), since for the geometry used in the form of rectilinear trenches the equation can be reduced to an ODE.
Finally, it may be interesting to consider nonlinear extensions to the differential equation (2.8) proposed, since we have only considered nucleation and evaporation ratios proportional to the density of adatoms, as well as the effects for other types of geometries as seen in Figure (2.8).

5 Conclusion

In this work we have proposed a simple model to numerically find out the growth of semiconducting nanowires in selective area epitaxy. The model is based in a partial differential equation built upon the steady-state second Fick law, with additional sink and source terms corresponding to the elements supposed to appear in selective area epitaxy.

The equation has been solved by means of the finite element method employing a Python library, and the results have been analysed for different values of the ratios and values of the parameters in the mask and trenches. The results obtained allowed us to understand the role of each of the parameters and provided us with qualitative information on the different growth regimes that can occur in this model. Essentially, the type of regime has turned out to depend mainly on the density of adatoms in each of the surface regions. The role of diffusion as well as of nanowire separation is to amplify the strength of these regimes, that is, the relative difference between the peak heights of the nanowires. However, they are not able to change the type of regime observed because they do not have an influence on the direction of the diffusion of particles between mask and trenches, only on its intensity.

It may be possible that these mechanisms play a role in actual nanowire growth processes and therefore that the dynamics shown in this simple model provide qualitative information about the regimes observed experimentally. Most likely, the resemblance is not significant due to the simplicity of the model. However, there are many ways to improve the model and add more precise corrections, and this work can be mostly seen as a way of computationally approaching this type of problem, based on the solution of a differential equation for its subsequent study.

What is really important, and where the physics lies, is in the postulated differential equation, that is, in the model. Therefore, the accuracy of the results will depend above all on postulating a differential equation that correctly captures what happens in a real nanowire growth process.

Bibliography

[1] J. Johansson et al. “Combinatorial Approaches to Understanding Polytypism in III–V Nanowires”. In: *ACS Nano* (2012). DOI: https://doi.org/10.1021/nn301477x.

[2] P. Yu et al. “Design and fabrication of silicon nanowires towards efficient solar cells”. In: *Nano Today* (2016). DOI: https://doi.org/10.1016/j.nantod.2016.10.001.

[3] S. Eaton et al. “Semiconductor nanowire lasers”. In: *Nat Rev Mater* (2016). DOI: https://doi.org/10.1038/natrevmats.2016.28.

[4] A Yu Kitaev. “Unpaired Majorana fermions in quantum wires”. In: *Phys.-Usp* (2001). DOI: http://iopscience.iop.org/1063-7869/44/10S/S29.

[5] K. Basset et al. “Teoria simmetrica dell elettrone e del positrone”. In: *Il Nuovo Cimento* (1937).

[6] R. Baxter. “Evolution of GaAs nanowire geometry in selective area epitaxy”. In: *Appl. Phys. Lett* (2015). DOI: https://aip.scitation.org/doi/10.1063/1.4916347.

[7] A Yu Kitaev. “Fault-tolerant quantum computation by anyons”. In: *Annals of Physics* (2002).

[8] V. Mourik et al. “Signatures of Majorana Fermions in Hybrid Superconductor-Semiconductor Nanowire Devices”. In: *Science Mag* (2012).

[9] P. Haining et al. “Disorder effects on Majorana zero modes: Kitaev chain versus semiconductor nanowire”. In: *Mesoscale and Nanoscale Physics* (2020). DOI: https://doi.org/10.1103/PhysRevB.103.224505.

[10] P Fendley. “Parafermionic edge zero modes in Zn-invariant spin chains”. In: *J. Stat. Mech* (2012).

[11] K. Basset et al. “Evolution of GaAs nanowire geometry in selective area epitaxy”. In: *Appl. Phys. Lett.* (2015).

[12] M. Borgstrom et al. “Synergetic nanowire growth”. In: *Nature Nanotechnology* (2007). DOI: doi:10.1038/nnano.2007.263.

[13] B. Goldstein. “Diffusion in Compound Semiconductors”. In: *Physical Review* (1960).

[14] S. Jiang et al. “Selective area growth of InP in shallow trench isolation on large scale Si(001) wafer using defect confinement technique”. In: *Journal of Applied Physics* (2013). DOI: https://doi.org/10.1063/1.4815959.

[15] URL: https://www.sciencedirect.com/topics/engineering/diffusion-length.

[16] URL: https://fenicsproject.org/.

[17] Y. Wang et al. “Surface Reaction Kinetics of InP and InAs Metalorganic Vapor Phase Epitaxy Analyzed by Selective Area Growth Technique”. In: *Japanese Journal of Applied Physics* (2008). DOI: DOI:10.1143/JJAP.47.7788.

A Characterizations of the parameters

In this appendix, we will approach whether the ratios between the parameters in the mask and the trench should be used to best describe the system, or if on the other hand we should use their absolute value. This may seem like a nuance, however it helps to better understand the role of each parameter. To that end, we want to figure if the influence of each parameter is mostly due to the relative strengths between the mask and the trench or if, on the other hand, it is due to their value.

To figure this out, we plot the observable r fixing all of the parameters except one of them, on both the mask and the trenches. If the absolute value at both regions contributes to the regime more than the corresponding relative strength, then it is better to vary the absolute value, while if the relative strength dominates the behaviour, then using the ratios is justified.

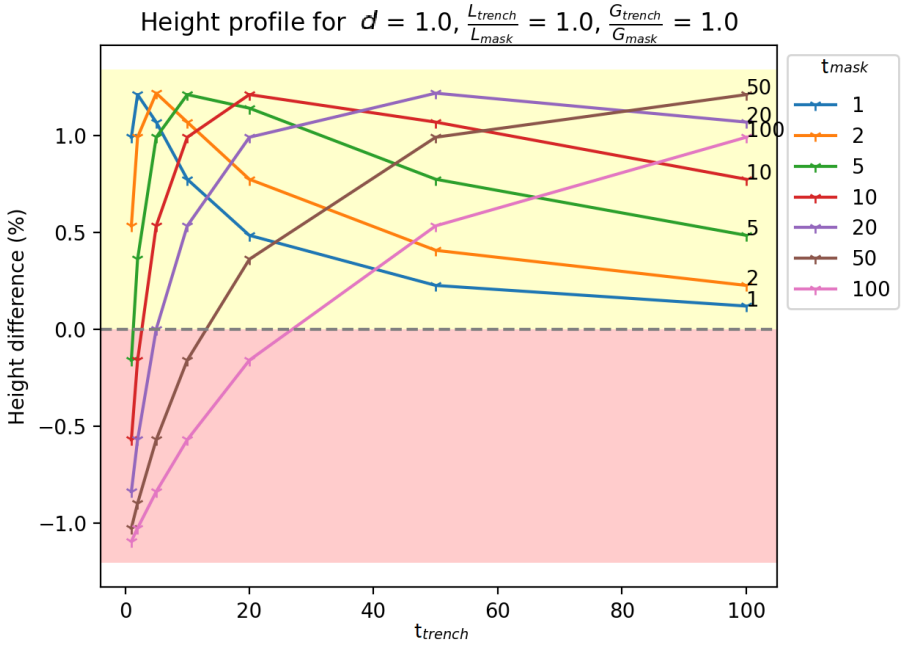

Figure A.1: Observables fixing all the parameters except the characteristic times

First of all, on Figure (*A*.1) we can see the influence of the characteristic time on the system after fixing the rest of the parameters. We can see how the relative strength between the values of t at the mask and the trenches matter more than its absolute value. The value of the ratios produces a very strong effect on the solution, although the origin of this effect is unknown to us. Because of this, we find it necessary to capture this behaviour in the solutions in the results section by using the ratio between t instead of its

absolute value.

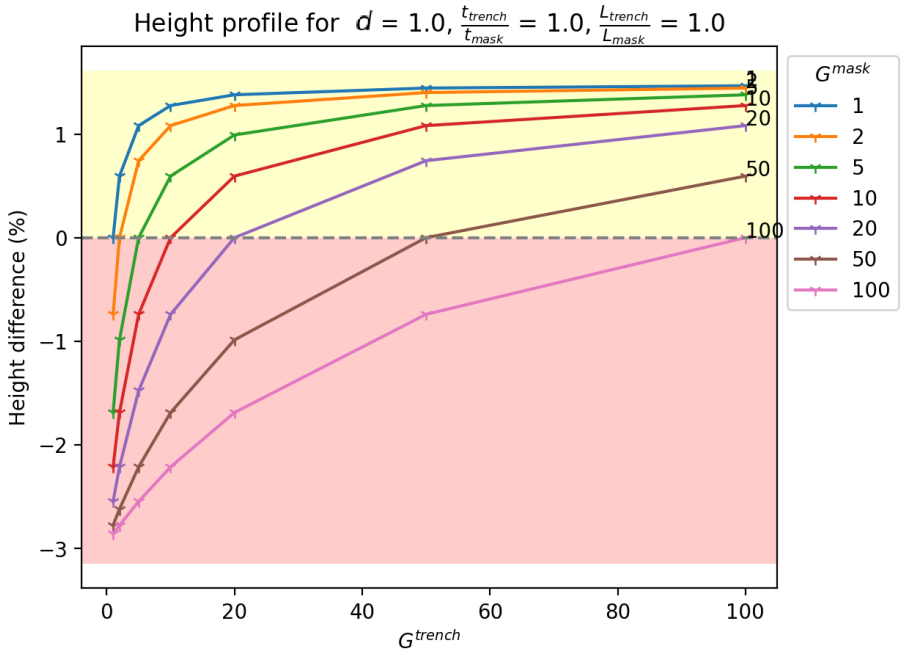

Figure A.2: Observables fixing all the parameters except the input particle fluxes

Now, on Figure (*A*.2) we perform the same operation but for the input flux G. In this case, we see how the values of G in the mask and in the trenches produce opposite effects in the solution: increasing G in the trenches is equivalent to decreasing it in the mask. Therefore, we also find it convenient to use the ratios of G to capture this behavior in the results.

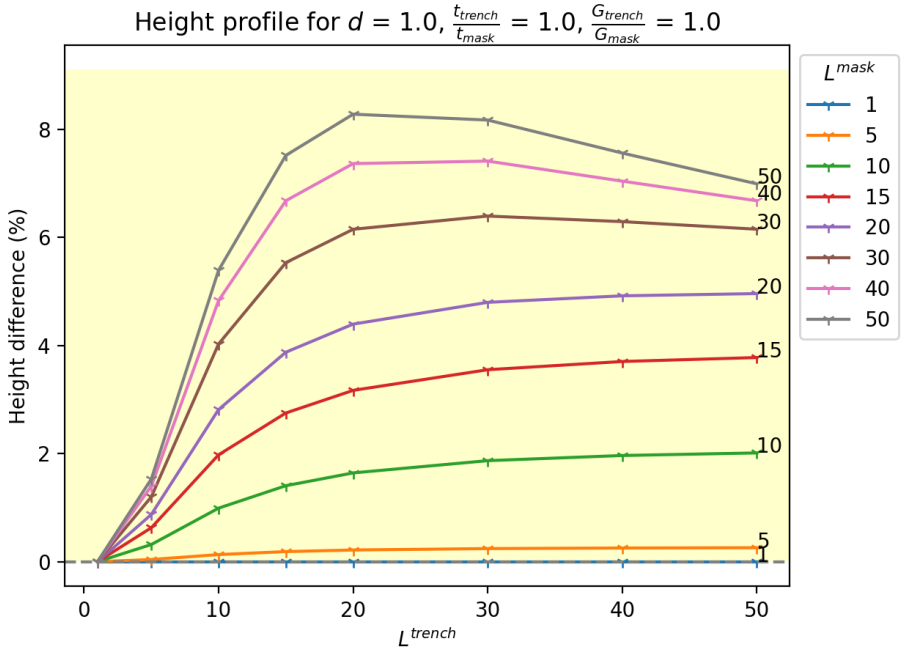

Figure A.3: Observables fixing all the parameters except the characteristic lengths

Finally, on Figure (*A*.3) we perform the same operation for the characteristic length L. In this case, the behaviour is no longer the same and the most important contribution comes from the absolute value of L. Indeed, we can see how increasing L at the trench of at the mask both help to increase or decrease the height difference between the wires. For this reason, we believe that the ratios for the characteristic length do not help to describe the growth regime and we will instead use its absolute value.